

Effects of Buoyancy on the Flowfields of Lean Premixed Turbulent V-Flames

R. K. Cheng, B. Bédard, D. T. Yegian
Environmental Energy Technologies Division
Ernest Orlando Lawrence Berkeley National Laboratory
MS70-108B, 1 Cyclotron Rd. Berkeley, CA 94720
RKCheng@lbl.gov

and

P. Greenberg
Microgravity Sciences Division
NASA Lewis Research Center
Cleveland, OH 44135

Abstract

Open laboratory turbulent flames used for investigating fundamental flame turbulence interactions are greatly affected by buoyancy. Though much of our current knowledge is based on observations made in these open flames, the effects of buoyancy are usually not included in data interpretation, numerical analysis or theories. This inconsistency remains an obstacle to merging experimental observations and theoretical predictions. To better understand the effects of buoyancy, our research focuses on steady lean premixed flames propagating in fully developed turbulence. We hypothesize that the most significant role of buoyancy forces on these flames is to influence their flowfields through a coupling with mean and fluctuating pressure fields. Changes in flow pattern alter the mean aerodynamic stretch and in turn affect turbulence fluctuation intensities both upstream and downstream of the flame zone. Consequently, flame stabilization, reaction rates, and turbulent flame processes are all affected. This coupling relates to the elliptical problem that emphasizes the importance of the upstream, wall and downstream boundary conditions in determining all aspects of flame propagation. Therefore, buoyancy has the same significance as other parameters such as flow configuration, flame geometry, means of flame stabilization, flame shape, enclosure size, mixture conditions, and flow conditions.

To characterize the field effects of buoyancy, our approach is to compare flames in normal gravity (+1g), reversed gravity (-1g) and in microgravity (μ g). μ g flames experiments are the key to reconcile the sometimes counter intuitive observations made in +1g and -1g flames. We have taken a relatively broad approach by conducting laboratory studies of the field effect of gravity on stabilization limits, flame wrinkle structures, and mean and rms velocities in several flame configurations. Exploration of many of these coupled phenomena is necessary to provide an overview and to build the foundation needed for defining the appropriate configuration and conditions for microgravity flight experiments. Our investigation of rod-stabilized v-flames subjected to +1g and -1g have led to the discovery of new turbulent flame phenomena [Bedat and Cheng, 1996] and to more open questions [Bedat, Cheng and Kostiuik, 1999]. In particular, we found that the effects of buoyancy in turbulent flames persist beyond the limit predicted by current scaling laws.

The phenomenon was first shown by the mean v-flame angles, α . This mean flame property of +g, -g and μ g flames should converge with increasing flow momentum. Simple scaling argument suggests that the limit would be around Richardson number $Ri < 0.1$. For laminar +1g and -1g flames, convergence was found at $Ri < 0.2$ ($Re > 2000$). For turbulent flames, however, a convergence was not shown. Significant differences exist under flow conditions of $Ri < 0.2$ beyond the convergence limit determined for laminar flames. The results demonstrate that buoyancy influence on turbulent flames does not seem to diminish with increasing mean flow momentum. By the use of 2D Planar Laser Induced Fluorescence technique for OH radicals, we found that the difference is due to a difference in flame wrinkle structures. Under identical flow and mixture conditions, the -1g the turbulent flame is more wrinkled in the near field region adjacent to the stabilizer rod than the +1g flame.

To further understand how the differences in flame wrinkling relate to the velocity statistics, we use laser Doppler anemometry (LDA) to characterize the flowfields of +1g, -1g and μ g flames. LDA is a well-established diagnostics. Our laboratory two-component four beam LDA system uses a 4 watt Argon-Ion laser source. It is interfaced to a PC that also controls a three-axis traverse table to scan the flame automatically. It is obvious that this system is too complex for μ g experiments conducted on board an aircraft. To develop a LDA system for

parabolic flights, we took a two step approach in. Starting with a compact one-component LDA, the first goal was to demonstrate the feasibility of using LDA in aircraft experiments. The main concern was whether the optical system and its alignment would be sufficiently robust to withstand the varying g forces and vibration during the airplane pull-ups and parabolas. There were other issues such as proper seeding device and developing the experiment protocol to scan the flowfield. Based on the 1D LDA experience, a 2D-LDA system was designed and tested successfully in recent parabolic flights.

The experimental package (Figure 1) is a fully computerized self-contained apparatus that is design to accept different laser diagnostics. The burner is mounted on a two-axis computer controlled translating stage to position the laser probe relative to the flame. Fuel and air supplies are metered through two electronic flow controllers and mixed prior to entering the burner. The 1D LDA system is designed in a forward scattering configuration. The laser source is an external cavity-doubled diode pumped Nd:YAG laser outputting 14 milliwatts at 532 nanometers (Adlas DPY 205C). An equal-path BK-7 splitting prism is utilized, so that additional pathlength compensation elements are not required. The beams are brought to a focus with a 160 mm achromat, yielding a $1/e^2$ transverse probe volume dimension of approximately 150 microns. Scattered light is collected at 15 degrees off the forward scattered direction by a well corrected 55 mm, F/2.8 commercial camera lens. The probe volume is focused onto a 100 micron diameter multimode optical fiber. The signal is digitized by the input section of dedicated burst spectral processor (QSP M240S).

The 2D-LDA system constructed for the microgravity experiments uses a pair of semiconductor diode lasers each emitting 15 milliwatts at 676 and 780 nanometers, respectively. The two beam paths are arranged coaxially through the use of an over-center dove prism. Equal-path BK-7 beam splitters are employed for both components. Separate mode matching optics for each channel provide commensurate transverse probe volume dimensions of 90 microns with proper imaging of the beam waists. The scattered light is collected at 15 degrees off the forward scattered direction and a dichroic filter is used to separate the scattered signal into its component wavelengths. The twin images of the probe volume are focused onto the input facets of two 100 micron diameter multimode optical fiber. Variable bandpass analog anti-aliasing filters proceed digitizing by the input section of dedicated burst spectral processor (QSP M240S). The two transverse velocity components are angularly separated by 90° . The optical transmitter can be rotated around its optical axis to orient the component velocities relative to the axis of the burner. In the experiments described here, the individual components were arranged at $\pm 45^\circ$ relative to vertical. The algebraic combination of the outputs directionally resolves the radial velocity providing that there are no flow reversals in the axial direction.

Measurements of velocity statistics in μg flames involve rather complex experimental protocol. Fortunately, the LDA systems we have designed and built was sufficiently robust such that re-alignment was not necessary between parabola or flights. During the short time of each parabola (about 30 sec pullup, 15 sec. microgravity), the follow steps were executed : 1) purge the burner, 2) set the fuel and air flow rates, 3) ignite the flame, 4) traverse the burner to a pre-assigned position, 5) trigger the LDA measurements, 6) record gravitational levels, 7) turn off the flame and 8) return the burner to its park position. Consequently, each parabola allowed measurements at only one position.

Figure 2 compares the 2D velocity vectors obtained in $+1g$ and $-1g$ laminar flames at $Re = 1250$. Under this low velocity condition, there are significant differences in the flame shapes and in their flowfields. In $+1g$, flow acceleration is observed in the products but in $-1g$ constant deceleration is found. The stagnation point and the outer flow circulation zone of the $-1g$ flame are also apparent.

Though the outline of the turbulent flame brushes indicate that the $-g$ turbulent flame in Figure 3 is broader and shorter than the corresponding $+g$ flame, differences in the velocity vectors are much less noticeable. Due to the high flow velocity, the stagnation point of $-1g$ flames is beyond our measurement domain. Starting at $x < -40$ mm, there is a very slight deceleration within the products of the $-1g$ flame. The velocity vectors also show a more divergent flow compared to the $+1g$ case. This is consistent with the change in mean radial pressure gradient. Whether or not this slight change can be responsible for the drastic change in flame wrinkle structure needs to be investigated more thoroughly. We are continuing the analysis of the velocity statistics, in particular measurement of conditional statistics being carried-out in the laboratory, would be very useful to determine if the changes in flame wrinkle structures has significant effects on flame generated turbulence.

Figure 3 compares centerline profiles of turbulent +1g and μg v-flames ($Re = 2500$ and $\phi = 0.65$). Each point of the μg velocity profile was collected during separate parabolas to ensure stable statistics. A lack of significant scatter in the data is a good indication that the experiments were highly reproducible. The most interesting finding is that in μg the mean axial velocities are only half as high as those measured in +1g flames. This is rather surprising because of the small differences in the velocities shown between the +1g and -1g flames. Measurements made in a laminar μg v-flame also show similar velocity reduction. Whether the differences are associated with significant re-distributions in the flowfields will be shown when the data obtained by the use of the 2D-LDA system are fully analyzed. These results illustrate again the value of μg experiments for without them, the true nature of buoyancy on flame propagation would be difficult to reveal.

References

Bedat, B. and Cheng, R. K., (1996) "Effects of Buoyancy on Premixed Flame Stabilization" *Combustion and Flame*, 107, 13-26.

Cheng, R. K., Bedat, B., Kostiuk, L. W. (1999) "Effects of Buoyancy on Lean Premixed V-Flames: Part I: Laminar and Turbulent Flame Structures, *Combustion and Flame*, 116.

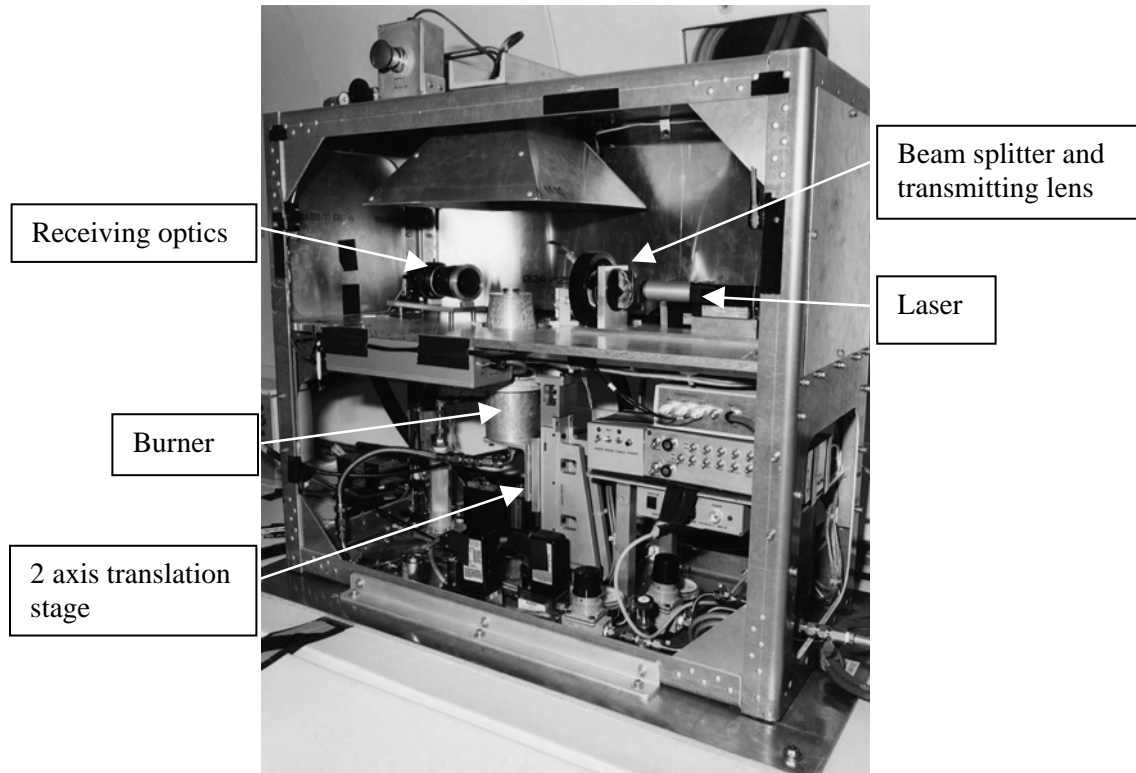


Figure 1 Experimental package for aircraft experiment showing the LDA optics on the middle platform

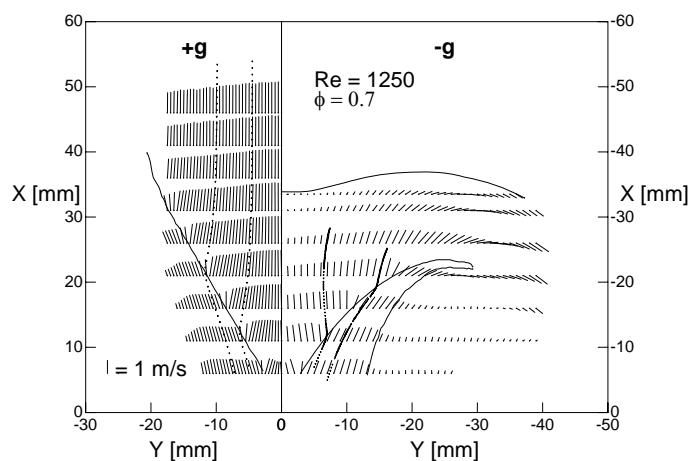


Figure 2 Comparison of 2D velocity vectors measured in a +1g laminar v-flame (left side) and a -1g laminar v-flame (right side)

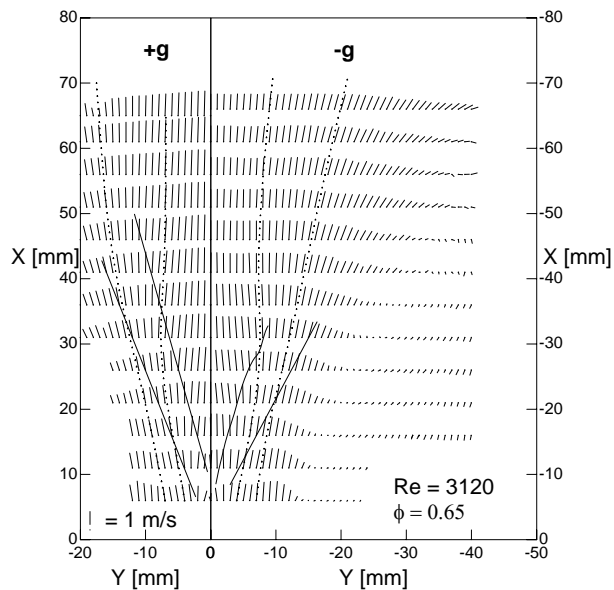


Figure 3 Comparison of 2D velocity vectors measured in a +1g turbulent v-flame (left side) and a -1g turbulent v-flame (right side)

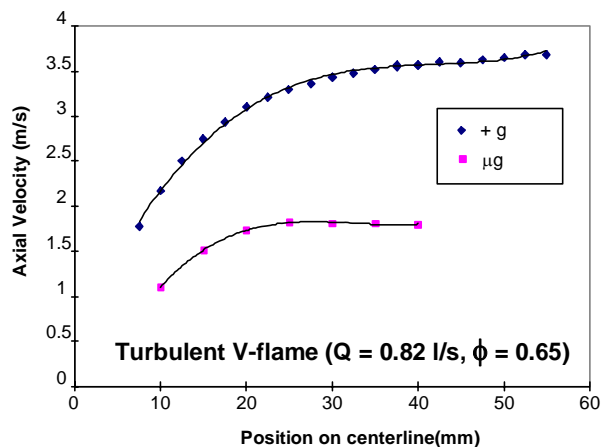


Figure 4 Comparison of axial velocity profiles at the centerline of a turbulent v-flame in +1g and in μg